Applied Physics Letters

Magnetic characteristics of phase-separated CeO_2:Co thin films

Cite as: Appl. Phys. Lett. **103**, 102409 (2013); https://doi.org/10.1063/1.4820145
Submitted: 20 June 2013 . Accepted: 20 August 2013 . Published Online: 06 September 2013

M. C. Prestgard, G. Siegel, Q. Ma, and A. Tiwari

Magnetic characteristics of phase-separated CeO_2:Co thin films

M. C. Prestgard,[1] G. Siegel,[1] Q. Ma,[2] and A. Tiwari[1,a)]
[1]*Nanostructured Materials Research Laboratory, Department of Materials Science and Engineering, University of Utah, Salt Lake City, Utah 84112, USA*
[2]*DND-CAT, Northwestern Synchrotron Research Center at the Advanced Photon Source, Argonne, Illinois 60439, USA*

(Received 20 June 2013; accepted 20 August 2013; published online 6 September 2013)

Herewith, we are reporting the magnetic properties of phase-separated Co-doped CeO_2 films (with a Ce:Co atomic-ratio of 0.97:0.03) grown on single-crystal $SrTiO_3$ (001) substrates. A comparison of the magnetic characteristics of these films with those of homogenously doped CeO_2:Co films of the same composition illustrates the significant differences in their magnetic behavior. These behavioral characteristics provide a model for determining if the magnetic behavior observed in this, as well as in other diluted magnetic dielectric systems, is due to homogeneous doping, a mixture of doping and transition metal cluster formation, or exists purely as a result of transition metal clustering. © *2013 AIP Publishing LLC*. [http://dx.doi.org/10.1063/1.4820145]

The miniaturization of devices is the main driving force for the development of the electronics industry and occurs with predictable regularity in accordance with Moore's law.[1,2] This miniaturization, however, is approaching a limit; one defined by the fact that the efficiency of current devices is physically constrained by material properties at such sizes. In order to overcome this hurdle, alternative facets of technological improvement other than miniaturization must be considered. One such area is spintronics, which allows the utilization of an electron's spin in addition to its charge.[3–6]

Spintronic devices can be classified in two groups, active devices and passive devices. Though passive spintronics have been quite successful in their various applications, such as magnetic read-heads, magnetic RAM, etc., active spintronic devices are essential for this technology to advance further.[3,4] Realization of active spintronics requires the injection and manipulation of electrons' spins in semiconductors. Initial spin injection attempts showed serious limitations in efficiency, as material mismatches existed between the metallic ferromagnet used to inject the electrons and the semiconductor used as the base of the device.[7,8] Diluted magnetic semiconductors (DMS) have likewise been attempted for spin injection; however, overall low Curie temperatures have once again resulted in limited success.[9,10] Another potential route for injecting spin polarized carriers into semiconductors is by using ferromagnetic tunnel barriers, which can act as a spin filter and allow only one kind of spin to tunnel into the semiconductor.[11–15] The feasibility of spin dependent tunneling has been demonstrated using europium chalcogenides (EuX, X: O, S, Se).[16,17] However, europium chalcogenides exhibit a T_c that is much lower than room temperature, making them useless for practical device applications. In order to be useful in real applications, the spin filter material needs to be ferromagnetic at room temperature.

Recent reports of the observation of room temperature ferromagnetism (RTF) in dilute magnetically doped dielectrics (DMD) have created a lot of excitement in the field.[18–20] Cobalt doped CeO_2 is one of the most widely studied members of this family. It has been shown that when a small amount (~3 at. %) of cobalt replaces Ce in CeO_2, the material exhibits RTF. Although the above reports have generated a lot of enthusiasm among spintronic researchers, they also raised some doubts about whether the observed behavior is an intrinsic property of the material or due to some kind of precipitates. To clarify this aspect, more studies utilizing state-of-the-art techniques of elemental determination are needed. In this paper, we are reporting the growth, characterization, and magnetic properties of phase-separated cobalt-doped CeO_2 films in order to better understand the behavioral differences between this and the homogeneously doped CeO_2 films.

The phase separated CeO_2:Co films (with a Ce:Co atomic-ratio of 0.97:0.03) were prepared using a pulsed laser deposition (PLD) system. A traditional sol-gel technique was used to prepare CeO_2:Co powder. This was followed by subsequent sintering and iso-static pressing to generate a highly dense ceramic pellet for laser ablation. A Lambda Physik Compex Pro KrF excimer laser ($\lambda = 248$ nm and pulse width of 25 ns) was used to ablate the dense ceramic target at a pulse repetition rate of 10 Hz. The deposition was performed under an oxygen deficient environment (base vacuum of 10^{-5} mbar) to deliberately induce cobalt precipitation in the system. The ablated material was deposited on single crystal STO (001), which was heated to 650 °C during the deposition. The deposition rate, as determined using a P-10 Tencor profilometer, was found to be approximately 0.47 Å/shot, thus, 11 000 laser pulses resulted in a film of thickness of approximately 520 nm.

A Philips X'Pert X-ray Diffractometer (Cu Kα radiation) was used for X-ray diffraction (XRD) measurements. X-ray photoelectron spectroscopy (XPS) was performed using a Kratos Axis Ultra DLD. A Quantum Design superconducting quantum interference device (SQUID) was used to perform magnetic property measurements at temperatures between 10 K and 350 K. Synchrotron X-ray absorption spectroscopy (XAS) measurements were performed at the 5BM-D beamline of the DND-CAT at Sector 5 of the Advanced Photon

a)Email: tiwari@eng.utah.edu

Source (Argonne, IL). The Co K edge XAS measurements of the film samples were carried out in fluorescence mode by collecting the Co Kα emission intensity using a 4-element Si-drift solid state detector (SII NanoTechnology). The film sample was mounted vertically on a spinner with its surface normal bisecting the 90° angle between the X-ray incidence and photon detecting directions. The film sample spins during data collection to minimize Bragg diffraction from the substrate. A double crystal Si (111) monochromator was used for energy selection. The incident X-ray intensity was detuned by 65% for harmonic rejection. Bulk reference data were collected in transmission mode on metal Co foil and powder CoO and Co_2O_3. Fine CoO and Co_2O_3 powders were uniformly spread on long Scotch tape (3M Corp) which were then folded to produce adequate absorption. The Athena and Artemis software packages were used for XAS data analyses.

Figure 1 shows the XRD pattern for a CeO_2:Co thin film along with that for a pure STO substrate. Only the peaks corresponding to the (200) and (400) orientations of the parent CeO_2 could be observed, indicating c-axis oriented growth. This result is consistent with the growth mechanism previously reported for CeO_2 based systems.[18,21] The presence of cobalt could not be definitively determined by XRD, as the amount of doping was very small, and moreover, the anticipated cobalt peaks overlap the STO peaks, specifically those near 41.7° and 47.6°. In order to evaluate the state of cobalt in the film, further characterization was performed using an XAS technique.

Figure 2 shows XAS results for CeO_2:Co thin films. The experimentally observed XAS spectra are shown in Figure 2(a), while Figures 2(b) and 2(c) show the k-space and the R-space Fourier transformation, respectively. We have also shown the data collected for Co metal, Co_2O_3, and CoO in the above figures. These standards were all used in a linear combination fit (LCF) model, using Athena.[22] The LCF modeled the Co K-edge data from the doped sample as a combination of pure cobalt and cobalt of varying oxidation states (pure cobalt—Co^0, CoO—Co^{2+}, and Co_2O_3—Co^{3+}). The best fit of these three models indicated that of the 3% cobalt dopant, 85.7% (±0.7%) was in metallic precipitate form, 12.6% (±0.9%) was in Co^{3+} form, and 1.7% (±0.5%) was in Co^{2+}.

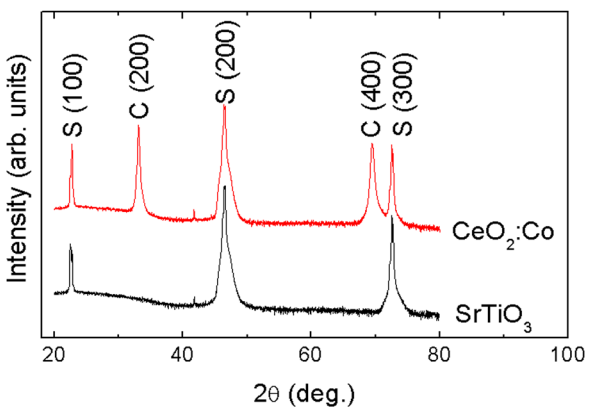

FIG. 1. X-ray diffraction patterns for the CeO_2:Co film and the STO substrate. The S peaks correspond to substrate, whereas the C peaks correspond to CeO_2. No cobalt peaks could be detected.

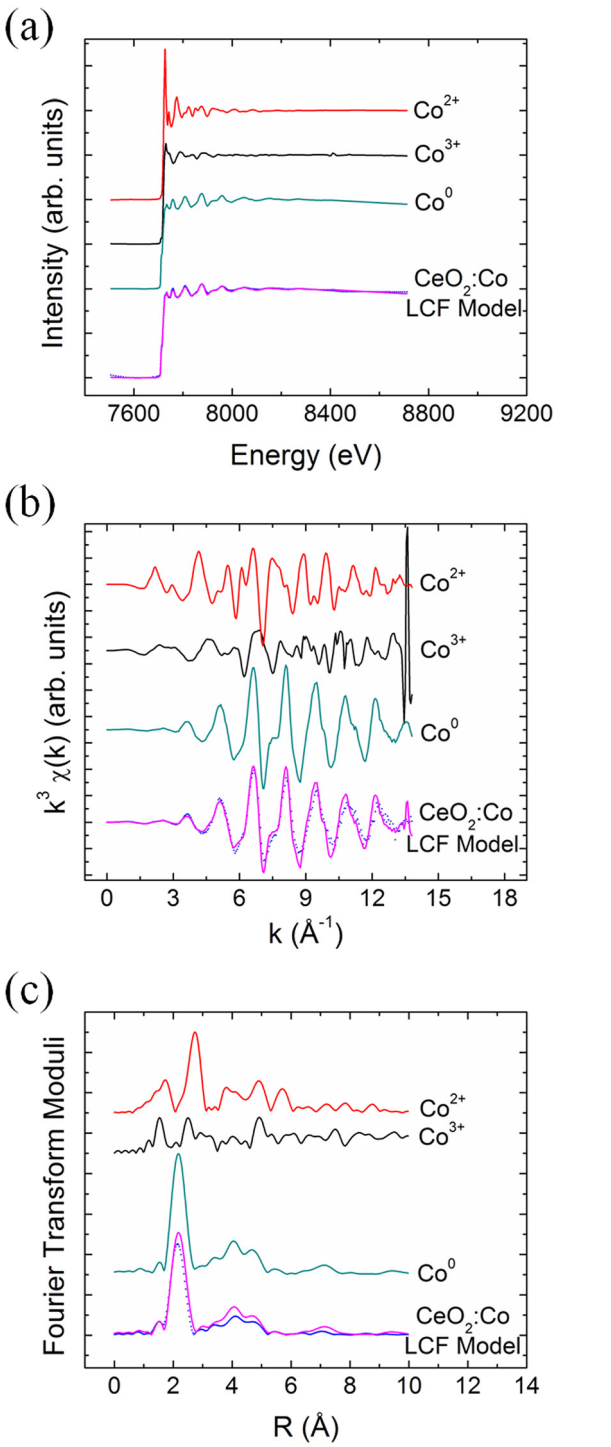

FIG. 2. (a) X-ray absorption spectroscopy data for the Co K-edge of CeO_2:Co film deposited on STO (blue curve). Also shown is a fit to LCF model (purple curve) along with the standard data for CoO, Co_2O_3, and Co metal, (b) K-space and (c) R-space Fourier transform for each of the above data.

XAS studies were supplemented by the XPS. Figure 3 shows the $2p_{3/2}$ spectra of cobalt recorded from a CeO_2:Co film. De-convolution of this spectrum showed the presence of two sets of peaks, one at 778.3 eV and the other centered at around 780.4 eV. The peak at 778.3 corresponds to metallic Co while the peak around 780.4 eV corresponds to a mixture of Co^{2+} and Co^{3+}.[23,24] Quantitative analysis of the XPS data showed that about 85% (±1%) of the cobalt exists as

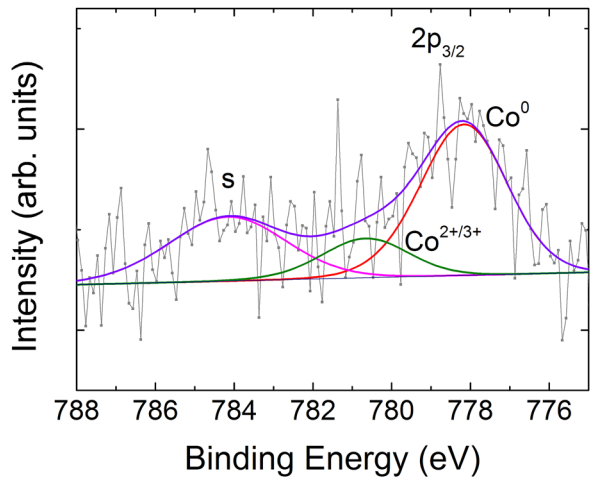

FIG. 3. XPS data for the CeO_2:Co film. The leftmost peak indicates a satellite peak. The peak at about 780.4 eV corresponds to $2p_{3/2}$ peak of the Co^{2+}/Co^{3+}. The peak at 778.3 eV corresponds to $2p_{3/2}$ peak of the metallic cobalt.

clusters, and the remaining 15% (±1%) is a mixture of the 2+ and 3+ valence states.

In Figures 4(a)–4(e), we have shown the magnetization *vs.* field (M *vs.* H) data for the CeO_2:Co films at different temperatures over the range of 10 K to 300 K. The M *vs.* H data show clearly visible hysteretic behavior at 10 K. A coercive field of ~850 Oe was observed at this temperature. The coercivity of the films dropped as the temperature was increased and almost vanished at 300 K. However, the M *vs.* H data still exhibited a saturation effect. Figure 4(f) shows the field-cooled (FC) and zero-field-cooled (ZFC) magnetization *vs.* temperature (M *vs.* T) data. The ZFC/FC M *vs.* T data show bifurcation at about 250 K. The observed behavior is a characteristic of a superparamagnetic system. A material exhibits superparamagnetism when it is comprised nanoscale magnetic clusters embedded in a nonmagnetic matrix.[25] So the magnetic results are consistent with the conclusions of XAS and XPS which unambiguously indicated the presence of magnetic clusters. An estimate of the size of superparamagnetic clusters was made using the relation[25] $KV = 25\,k_BT_B$, where K is the bulk anisotropy energy, V is the volume of the magnetic cluster, k_B is the Boltzmann's constant, and T_B is the blocking temperature where ZFC and FC shows bifurcation. Using the anisotropy energy (K) of Co (Ref. 26) as 4×10^6 erg/cm^3 and the experimentally determined value of T_B as 250 K, the approximate diameters of the precipitates was found to be ~7.4 nm.

Quantitative analysis of the data revealed that the magnetic response of the system is much more complex than expected from a simple system comprising magnetic clusters embedded in a non-magnetic matrix. Specifically, the observed saturation magnetization of the films is significantly higher than that expected for metallic cobalt. The films showed a saturation magnetization of 2.4 μ_B/Co at 10 K which is 41% higher than the value expected for metallic cobalt (1.7 μ_B/Co).[27] This indicates that apart from forming clusters, some cobalt is also substituting for Ce in the CeO_2 matrix. Furthermore, our results indicated that the cobalt ions which substitute Ce in the CeO_2 matrix result in much higher magnetization as compared to the cobalt clusters.

In order to understand the above aspect, we will have to revisit the earlier work reported for homogeneously doped CeO_2:Co system.[18] Specifically, in the above report, it was found that in the homogeneously doped CeO_2:Co system, the orbital angular momentum of the Co remains unquenched. Because of this, the orbital angular momentum and spin angular momentum add up, giving rise to a net angular momentum, $J = L + S = 4$, which results in a spontaneous magnetic moment of $M \sim 6.7\,\mu_B$ per cobalt ion [$M = g\,\mu_B \sqrt{J(J+1)}$; $g = 3/2$, $J = 4$].[18,28] By assigning a moment of 1.7 μ_B/Co to metallic cobalt precipitates and a moment of 6.7 μ_B/Co to cobalt ions substituting Ce in CeO_2 matrix, we estimated a net magnetization of 2.45 μ_B/Co (±0.05) for the phase separated CeO_2:Co films based on the XPS and XAS results. This estimated value matches very well with the experimentally determined value of 2.4 μ_B/Co.

In summary, we have shown that when CeO_2:Co films are deposited under low oxygen pressure using a PLD system, it results in a phase-separated system, as shown by XAS and XPS. These techniques revealed that in this phase-separated system, approximately 85% of the cobalt exists as clusters, while the rest substitutes into the CeO_2 lattice. Phase-separated CeO_2:Co shows very unusual magnetic properties, which are very different from homogenously doped films as well as from a conventional superparamagnetic system. This variation in the anticipated behavior is due to there being two distinct contributions to magnetic moment; first, from the

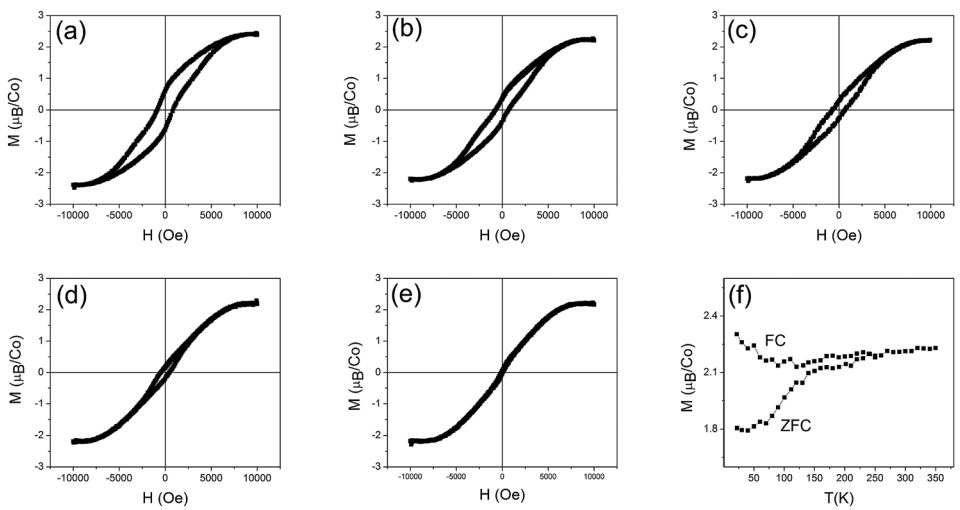

FIG. 4. M vs. H data for the phase separated CeO_2:Co films at (a) 10 K, (b) 50 K, (c) 100 K, (d) 200 K, and (d) 300 K. The figure (e) shows the ZFC and FC M vs. T data for the same film measured at H = 6000 Oe.

cobalt clusters present, and second due to the substitution of cobalt for cerium in the lattice. Detailed quantitative analysis of our results showed that the 60% of the total moment of the film originates from the 85% of the cobalt atoms that precipitate as metallic clusters while the remaining 40% of the total moment comes from just 15% of the cobalt that enters substitutionally in the CeO_2 matrix.

Financial support from NSF through Award No. 1121252 (CEMRI), Award No. DMR-0746486 (CAREER), and Award No. CMMI-1234338 is thankfully acknowledged. Research at DND-CAT was supported by E. I. DuPont de Nemours & Co., The Dow Chemical Company, and the State of Illinois. Use of the APS facilities was supported by the DOE's Office of Basic Energy Sciences, under the Contract No. DE-AC02-06CH11357.

[1]D. C. Brock and G. E. Moore, *Understanding Moore's Law: Four Decades of Innovation* (Chemical Heritage Foundation, Philadelphia, 2006), p. 25.
[2]P. S. Peercy, Nature **406**, 1023 (2000).
[3]S. A. Wolf, D. D. Awschalom, R. A. Buhrman, J. M. Daughton, S. von Molnár, M. L. Roukes, A. Y. Chtchelkanova, and D. M. Treger, Science **294**, 1488 (2001).
[4]G. A. Prinz, Science **282**, 1660 (1998).
[5]W. K. Park, R. J. Ortega-Hertogs, J. S. Moodera, A. Punnoose, and M. S. Seehra, J. Appl. Phys. **91**, 8093 (2002).
[6]S. J. Pearton, C. R. Abernathy, G. T. Thaler, R. M. Frazier, D. P. Norton, F. Ren, Y. D. Park, J. M. Zavada, I. A. Buyanova, W. M. Chen, and A. F. Hebard, J. Phys.: Condens. Matter **16**, R209 (2004).
[7]S. Datta and B. Das, Appl. Phys. Lett. **56**, 665 (1990).
[8]S. Das Sarma, J. Fabian, X. Hu, and I. Zutic, IEEE Trans. Magn. **36**, 2821 (2000).
[9]Y. Q. Song, H. W. Zhang, Q. Y. Wen, Y. X. Li, and J. Q. Xiao, Chin. Phys. Lett. **24**, 218 (2007).
[10]T. Fukumura, Y. Yamada, H. Toyosaki, T. Hasegawa, H. Koinuma, and M. Kawasaki, Appl. Surf. Sci. **223**, 62 (2004).
[11]X. Hao, J. S. Moodera, and R. Meservey, Phys. Rev. B **42**, 8235–8243 (1990).
[12]I. V. Shvets, A. N. Grigorenko, K. S. Novoselov, and D. J. Mapps, Appl. Phys. Lett. **86**, 212501 (2005).
[13]E. Y. Tsymbal, O. N. Mryasov, and P. R. LeClair, J. Phys.: Condens. Matter **15**, R109 (2003).
[14]R. Fiederling, M. Keim, G. Reuscher, W. Ossau, G. Schmidt, A. Waag, and L. W. Molenkamp, Nature **402**, 787–790 (1999).
[15]J. G. Simmons, J. Appl. Phys. **34**, 2581–2590 (1963).
[16]G.-X. Miao, M. Muller, and J. S. Moodera, Phys. Rev. Lett. **102**, 076601 (2009).
[17]A. Schmehl, V. Vaithyanhathan, and A. Hermberger, Nature Mater. **6**, 882–888 (2007).
[18]A. Tiwari, V. M. Bhosle, S. Ramachandran, N. Sudhakar, J. Narayan, S. Budak, and A. Gupta, Appl. Phys. Lett. **88**, 142511 (2006).
[19]P. Slusser, D. Kumar, and A. Tiwari, JOM **63**, 25 (2011).
[20]S. Kumar, Y. J. Kim, B. H. Koo, H. Choi, and C. G. Lee, IEEE Trans. Magn. **45**, 2439 (2009).
[21]J. F. Kang, G. C. Gong, G. J. Lian, Y. Y. Wang, and R. Q. Han, Solid State Commun. **108**, 225 (1998).
[22]S. Gautam, S. Kumar, P. Thakur, K. H. Chae, R. Kumar, B. H. Koo, and C. G. Lee, J. Phys. D: Appl. Phys. **42**, 175406 (2009).
[23]J. F. Moulder, W. F. Stickle, P. E. Sobol, and K. D. Bomben, *Handbook of X-Ray Photoelectron Spectroscopy* (Perkin-Elmer, Eden Prairie, MN, 1992).
[24]M. C. Biesinger, B. P. Payne, A. P. Grosvenor, L. W. M. Lau, A. R. Gerson, and R. St. C. Smart, Appl. Surf. Sci. **257**, 2717 (2011).
[25]C. P. Bean and J. D. Livingston, J. Appl. Phys. **30**, 120S (1959).
[26]N. W. Gray and A. Tiwari, J. Appl. Phys. **110**, 033903 (2011).
[27]V. S. R. Murthy, A. K. Jena, K. P. Gupta, and G. S. Murty, *Structure and Properties of Engineering Materials* (Tata McGraw-Hill Education, New Delhi, 2003).
[28]N. W. Ashcroft and N. D. Mermin, *Solid State Physics* (Harcourt College Publishers, Fort Worth, TX, 1975).